

The influence of metallurgy on the formation of welding aerosols†

Anthony T. Zimmer

National Institute for Occupational Safety and Health, Robert A. Taft Laboratories, MS-R3, 4676 Columbia Parkway, Cincinnati, OH 45226, USA

Received 5th March 2002, Accepted 24th July 2002

First published as an Advance Article on the web 27th August 2002

Recent research has indicated that insoluble ultrafine aerosols (*i.e.*, particles whose physical diameters are less than 100 nm) may cause adverse health effects due to their small size, and that toxicological response may be more appropriately represented by particle number or particle surface area. Unfortunately, current exposure criteria and the associated air-sampling techniques are primarily mass-based. Welding processes are high-temperature operations that generate substantial number concentrations of ultrafine aerosols. Welding aerosols are formed primarily through the nucleation of metal vapors followed by competing growth mechanisms such as coagulation and condensation. Experimental results and mathematical tools are presented to illustrate how welding metallurgy influences the chemical aspects and dynamic processes that initiate and evolve the resultant aerosol. This research suggests that a fundamental understanding of metallurgy and aerosol physics can be exploited to suppress the formation of undesirable chemical species as well as the amount of aerosol generated during a welding process.

Introduction

It has been estimated that there are over 800,000 workers employed as full-time welders.¹ Welding processes involve more than 80 different types, and each uses a wide variety of alloys and fluxing agents to protect both the substrate and welding alloy from chemical oxidation.² Welding operations produce gaseous and aerosol by-products composed of a complex array of metals, metal oxides, and other chemical species volatilized from either the base metal substrate, the welding alloy or the fluxing compounds.^{1,3,4}

Welding processes are known to generate high fume formation rates (FFR) with values typically ranging from 1.7–8.3 mg s⁻¹.^{5–8} In light of mass-based occupational safety and health standards, prior welding research has primarily focused upon characterizing how various welding parameters affect the FFR to indicate the relative “cleanliness” of a welding process.

Recent published research has indicated that for some classes of material (notably materials leading to aerosol particles with low solubility), biological activity following inhalation may be more appropriately represented by a lower moment of the particle size distribution (*e.g.*, aerosol number or surface-area concentration).^{9–11} As the particle number or surface-area per unit mass increases with decreasing particle size within an aerosol, the presence of sub-micrometer particles within the aerosol becomes increasingly significant as exposure metrics other than mass are considered. As will be discussed, the nature of welding processes results in the formation of ultrafine aerosols (*i.e.*, particles with physical diameters less than 100 nm).

The focus of this work is to demonstrate the fundamental importance of metallurgy in forming welding aerosols by presenting the dynamic aerosol formation mechanisms that create the resultant fume. The metal vapors emanating from the welding process serve as the feed material for aerosol formation. As the metal vapors chemically react and cool, particles are initially formed through nucleation. Aerosol growth processes, such as condensation and coagulation, will result in the subsequent growth of the nucleated particles. The influence of welding metallurgy will be tied to each of these

dynamic steps to illustrate how ultrafine aerosols are formed during welding processes.

Aerosol formation mechanisms and discussion

Metal vapor generation and chemical reactions

Torch and plasma welding operations generate metal vapors because the filler alloys and metal substrates reach temperatures that are sufficient to change their phase from a solid to a liquid. Metal vapors will diffuse away from the molten metal surface to the gas phase. Transport of vapors away from the molten surface will be facilitated by high temperatures and high vapor pressure metallic species. Additionally, chemical reactions (*e.g.*, reaction of the metal with oxygen in the surrounding environment) will also tend to increase the flux of metal vapor away from the metal liquid.¹²

If the metallurgy of the welding process is simple, probable chemical species can be inferred. However, welding processes are typically complex and involve numerous elements within the metallurgical mixture. To assist in predicting the phase and abundance of chemical species generated during industrial operations involving high-temperature processes, thermodynamic equilibrium analysis (TEA) can be used as a predictive assessment tool. This method minimizes Gibbs free energy (a standard thermodynamic variable), subject to constraints on the total number of moles of each element in the system.¹³ The high temperatures encountered during welding operations would tend to assist the equilibrium assumption in that reaction rates tend to vary exponentially with temperature.¹⁴

In several engineering applications, TEA has been successfully employed as a qualitative assessment tool in evaluating the form and phase of chemical species in environmental systems. Wu and Biswas¹⁵ used this technique to determine the speciation of metals among their various phases in an incinerator. Durlak *et al.*¹⁶ evaluated the role of process parameters on metallic emission rates. Owens *et al.*¹⁷ used this technique to determine the feasibility of using sorbents to control toxic metal emissions and to identify optimal operating regimes for maximal removal of metallic species.

Recently, Zimmer and Biswas¹⁸ used TEA to evaluate a braze welding alloy that is frequently encountered in occupational settings. This study provides an excellent example of the

†Presented at AIRMON 2002, Lillehammer, Norway, 3–7 February 2002.

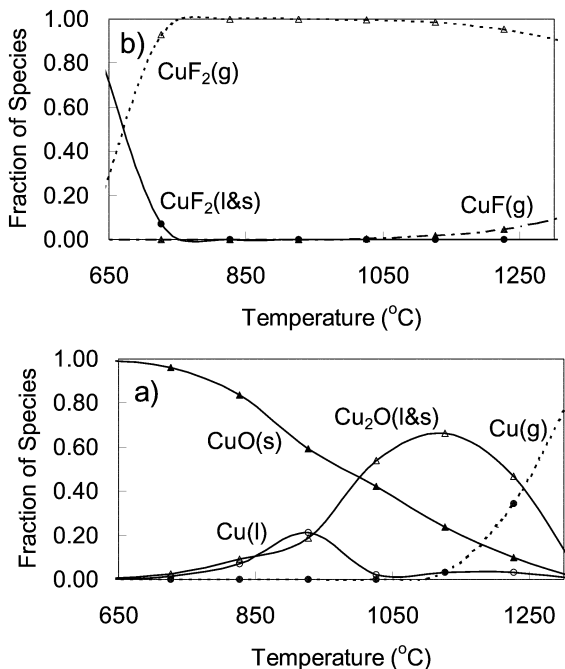


Fig. 1 Thermodynamic equilibrium analysis for the speciation of copper as a function of temperature when the self-fluxing brazing alloy is used (a) by itself and (b) with the supplemental fluxing compound.

role that fluxing compounds play on suppressing or promoting the formation of aerosols. A widely used, copper–phosphorus–silver brazing alloy (89% Cu, 6% P and 5% Ag) was selected for study. This alloy is self-fluxing with phosphorus playing the key metallurgical roles of lowering the alloy melt point and preventing oxidation reactions at the molten metal surface. When the base metals are dirty, this alloy can also be used with a supplemental fluxing compound (30–60% H₃BO₃, 25–40% KF₂, and 15–25% H₂O).

The TEA results were markedly different when comparing how copper reacted when used by itself and with the supplemental fluxing compound (Fig. 1a, b).¹⁸ The speciation of copper as a function of temperature for the self-fluxing alloy is presented in Fig. 1a. As demonstrated by this figure, the fluxing agent, phosphorus, appeared to have no effect on the partitioning (between the gas and condensed phases) of copper. At temperatures greater than 1250 °C, elemental copper is the dominant species while below this temperature copper oxides in the condensed form (*i.e.*, liquid or solid form) are thermodynamically favored. In contrast, when the brazing alloy elements were combined with the elements in the supplemental fluxing compound, copper was markedly affected by fluoride (Fig. 1b). The fluoride in the supplemental fluxing compound not only serves as a fluxing agent in reacting with oxygen, but also aggressively reacts with the metals found in the brazing alloy. At 650 °C, gaseous CuF₂ comprised 30% of the total rising to 100% of the total at 850 °C. It appears that fluoride serves to markedly reduce the temperature at which gas phase species become dominant.

The importance of the TEA analysis becomes readily apparent when comparing the aerosols that are formed when the brazing alloy is used by itself and when the brazing alloy is used in conjunction with the supplemental fluxing compound (Fig. 2).¹⁸ Samples were collected at ambient temperature using an experimental apparatus that allowed careful control of the time–temperature history as well as the dilution of the resultant aerosol. The scanning mobility particle sizer (SMPS, TSI Inc., St. Paul, MN, USA) was used to obtain particle size distribution measurements (weighed by particle number concentration) as a function of electrical mobility particle diameter. Fig. 2 illustrates the strikingly different behavior

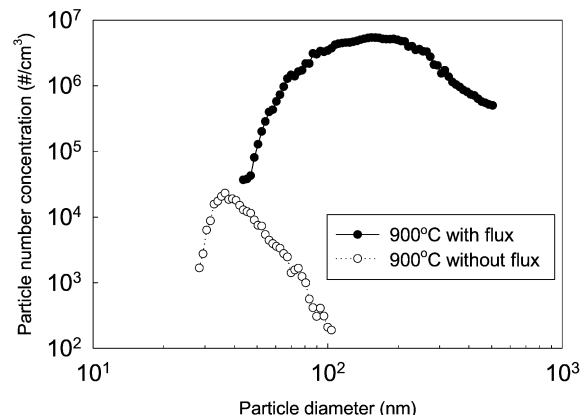


Fig. 2 Particle size distributions ($dN/d\log d_p$) measured using a scanning mobility particle sizer (configured with a long differential mobility analyzer) at 900 °C when the self-fluxing brazing alloy is used by itself and with the supplemental fluxing compound.

observed when the brazing alloy was heated by itself and in conjunction with the supplemental fluxing compound. The supplemental fluxing compound served to increase the production of aerosols over 500 times when comparing respective particle number concentrations.

Nucleation—Initial formation of particles from metal vapors

The high temperature metal vapors are transformed into primary particles through homogeneous nucleation. As the high-temperature metal vapors flux away from the welding torch or plasma, the temperature decreases to the point where the metal vapors become super-saturated. Thermodynamically, metal vapor species are no longer favored resulting in a phase transformation that creates an initial welding aerosol. Kinetic theory for gases can be used to derive the homogeneous nucleation rate (particles $s^{-1} cm^{-3}$) of the metallic species using the following equation:¹⁹

$$J = \left(\frac{2\sigma}{\pi m} \right)^{1/2} \frac{vN^2}{S} \exp \left[- \frac{16\pi}{3} \frac{v^2 \sigma^3}{(kT)^3 (\ln S)^2} \right] \quad (1)$$

where σ is the surface tension, m is the molecular mass, v is the molecular volume, N is the molecular number concentration of the vapor, S is the saturation ratio (defined as the partial pressure, p , divided by the saturation vapor pressure of the metal vapor, p_s), T is the absolute temperature, and k is the Boltzmann constant. Several items should be emphasized with regard to this equation. First, the nucleation rate is proportional to the square of the molecular number concentration. Secondly, the nucleation rate varies exponentially with the negative inverse cube of temperature (*i.e.*, high temperatures tend to increase the exponential function to its maximum value of 1).

Particle size distribution measurements illustrate how the nucleation rate is affected by the metallurgical conditions (Fig. 3).²⁰ Distribution measurement were obtained using a SMPS configured with a nano differential mobility analyzer (SMPS-NDMA, TSI Inc., St. Paul, MN, USA). Triplicate randomized air samples were collected during a gas metal arc welding operation using two shield gases, one composed of 100% CO₂, and the other 90% Ar/10% CO₂. The sample collection height was approximately 20 cm, and the sample collection temperature was approximately 22 °C. In comparing each shield gas condition, an increase in the carbon dioxide concentration results in roughly one order of magnitude increase in the particle number concentration for diameter less than 20 nm.

At this sample height, the 100% CO₂ shield gas condition appears to have nucleation and accumulation modes while the

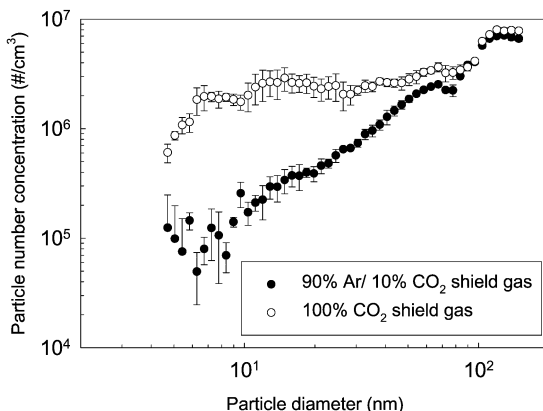


Fig. 3 Particle size distributions ($dN/d\log d_p$) measured using a scanning mobility particle sizer (configured with a nano differential mobility analyzer) for a gas metal arc welding (GMAW) process using (a) 90% Ar/10% CO_2 shield gas and (b) 100% CO_2 shield gas.

90% Ar/10% CO_2 appears only to have an accumulation mode (Fig. 3).²⁰ It appears that the 100% CO_2 shield gas condition facilitated higher nucleation rates. In this specific case, oxygen reacted with elemental iron (a major constituent of the welding alloy) to form iron oxide (*i.e.*, FeO), a substance with a significantly higher vapor pressure when compared to elemental iron. This reaction may have increased the mass transfer rate of elemental iron vapor from the molten liquid droplet resulting in a higher number concentration of metal vapor molecules. As given by eqn. (1), the higher number concentration of iron oxide vapor molecules would markedly increase the nucleation rate. TEA calculations support this hypothesis.²¹

Condensation—Particle growth due to additional metal vapors

Condensation is a dynamic process that serves to increase the size of the nucleated particles through transport of additional metal vapors onto the particle surface. To characterize the growth rate of an individual particle for diameters less than the mean free path, kinetic theory for gases can again be utilized to derive the following equation:²²

$$\frac{d(d_p)}{dt} = \frac{2m\alpha_c(p_\infty - p_d)}{\rho_p \sqrt{2\pi mkT}} \quad (2)$$

where d_p is the particle diameter, p_∞ is the partial vapor pressure well away from the particle, p_d is the vapor pressure at the particle surface (calculated using the Kelvin equation), and α_c is the condensation coefficient (an empirically derived value of 0.04 is frequently used). The other variables are the same as that in eqn. (1). One interesting point regarding this equation is that the particle growth in the free molecular regime is independent of the particle size and is driven primarily by the vapor pressure gradient between the bulk and the particle surface.

From a metallurgical standpoint, particle growth through condensation becomes important for metal alloys composed of volatile species with multiple vapor pressures. In the time-temperature history for the formation of a welding aerosol, chemical species with relatively low vapor pressures will be the first species to form particles through nucleation. At the temperatures that these species nucleate, the higher vapor pressure species will still exist as vapors. However, as time increases and the temperature decreases, the higher vapor pressure species will condense upon the freshly nucleated particles resulting in particle growth. The interesting result of particles that grow through condensation is the tendency to

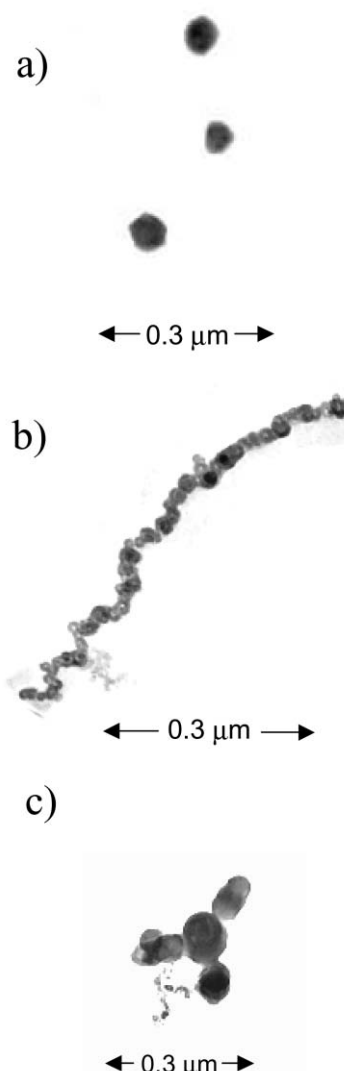


Fig. 4 Transmission electron microscope micrographs of representative welding aerosols for (a) braze welding, (b) gas metal arc welding, and (c) flux cored arc welding.

form “shelled particles” (*i.e.*, the chemical composition changes from the core to the surface of the particle).^{23–25}

An example of a welding aerosol that is condensation-growth dominated is shown by the transmission electron microscope (TEM, Philips, Model 420) micrograph from a braze welding process (Fig. 4a).¹⁸ TEM samples were collected by directing a slipstream to an Electrostatic Aerosol Sampler (TSI Inc., Model 3100). This aerosol resulted from heating the brazing alloy with the supplemental fluxing compound. The particles formed during this process were mainly spherical with diameters ranging from 50 to 300 nm.

Coagulation—Agglomerate growth through particle collisions

Coagulation is a dynamic aerosol growth mechanism where small particles collide to form larger agglomerates. These collisions may involve particle-particle, particle-agglomerate, or agglomerate-agglomerate interactions. If collisions occur between liquid particles, a single fused spherical particle may result. If collisions occur between solid particles, an agglomerate forms that is held together by van der Waals and other attractive forces (*i.e.*, electrostatic or magnetic forces). Collisions between partially molten particles could result in partially sintered agglomerates.

Unlike condensation, the mass of the aerosol is temporally conserved for coagulation. As time increases, the total number

concentration decreases while the particle size shifts to larger sizes. For monodisperse coagulation, the following equation gives a mathematical description for the change of number concentration with respect to time:²²

$$\frac{dN}{dt} = -\frac{4kTC_c\beta}{3\eta} N^2 \quad (3)$$

where N is the particle number concentration, C_c is the particle slip correction, η is the gas viscosity, and β is a concentration gradient correction factor. The other constants/variables are the same as described by eqn. (1). The key point regarding this equation is that the coagulation rate is proportional to the square of the particle number concentration. As such, coagulation occurs rapidly for high particle number concentrations.

Coagulation serves to increase the particle size. If coagulation occurs between liquid droplets, an analytical solution for the change in particle size at any time can be derived from derived from the preceding equation:²²

$$\frac{d(t)}{d_0} = \left(\frac{N_0}{N(t)} \right)^{1/3} \quad (4)$$

where d_0 and N_0 are the original particle diameter and particle number concentration, respectively. Given this equation, an eightfold reduction in the particle number concentration will be required to double the particle size. If coagulation occurs between solid particles, eqn. (4) tends to under-predict the growth of these open-structured agglomerates.²²

A good example of a coagulation-dominated aerosol growth is given by a gas metal arc welding operation using an iron-based alloy (97–98% Fe) and inert gas shielding (90% Ar, 10% CO₂) (Fig. 4b).²³ As demonstrated by the TEM micrograph (the sample was collected using a “cold-finger” technique and analyzed using a Philips Transmission Electron Microscope, Model 420), the aerosols formed during this process mainly result in homogenous, chain-like agglomerates. It appears that the dominant aerosol formation mechanisms during this process include nucleation of primary particles, followed by growth through coagulation. The chainlike nature of the aerosols generated by this process is probably related to the formation of primary particles composed primarily of magnetite (γ -Fe₃O₄) with magnetic forces dictating the simple linear structure of the agglomerates.

Competing aerosol growth mechanisms—Flux cored arc welding (FCAW)

The previous sections have given examples where condensation or coagulation is the dominant aerosol growth mechanism (Fig. 4a, b). However, certain welding operations and metallurgical conditions will result in strong competition between each growth mechanism. A representative example is given by the aerosols generated by a FCAW operation. Unlike a GMAW alloy that relies on a shield gas to protect the molten metal droplets within the plasma from oxidation, FCAW alloys employ fluxing compounds (e.g., alkali metals, fluoride) within the core of the wire to protect the alloy against oxidation.

The aerosols produced during FCAW alloy are heterogeneous and contain a mixture of chainlike and spherical structures (Fig. 4c). This finding suggests that nucleation of primary particles, composed primarily of magnetite, is followed by competing dynamic mechanisms including growth by coagulation and condensation of lighter elements onto the nucleated particles. Energy dispersive X-ray analysis (EDAX, Princeton Gamma-tech Avalon, Model 4000) of the FCAW aerosols supports this finding in revealing the presence of elements found in the GMAW process, as well as alkali metals such as magnesium, calcium, and barium.²³ These findings were also consistent with other studies.^{26,27} In addition to the equations previously discussed, characteristic time calculations

can be used to assess the relative importance of each aerosol formation mechanism.^{18,28}

Monitoring implications and conclusion

Assuming that particle number concentration or particle surface area may be the appropriate dose metric for ultrafine particles,^{9–11} gravimetric methods and direct reading instrumentation currently used for determining the particle size distribution may not adequately qualify/quantify ultrafine aerosols produced during welding processes. For example, assume a filter sample had been collected for elemental analysis of a GMAW process, and that welding occurred on a substrate contaminated with lead paint. Given its high vapor pressure, it is likely that lead vapor would condense late in the particle formation process resulting in a surface coating on fume primarily composed of iron. An elemental analysis could yield misleading results by showing that the percentage of lead was small in relation to the other elements. Research is currently being conducted to address this issue. Another monitoring implication regards particle size distribution measurements using direct reading instrumentation (e.g., aerodynamic particle sizer or optical particle counter). These instruments were designed to sample micrometer scaled particles, and have detection efficiencies that fall off rapidly for sub-micrometer particles.

The previous sections illustrated the influence of welding metallurgy on each aerosol formation step. The composition of the welding alloy and substrate, as well as the time-temperature history that evolves the welding fume are crucial factors in determining the relative importance of each aerosol formation mechanism. The particles that form during these processes may be composed primarily of spherical particles, as illustrated by the brazing aerosols (Fig. 4a). The particles that formed may also be open-structured agglomerates, as illustrated by the GMAW and FCAW aerosols (Fig. 4b, c). Additionally, the metallurgical aspects of the alloy and fluxing compounds can have a marked effect in promoting or suppressing the total particle number concentration (Fig. 2).

A final item to consider regards the deposition of ultrafine aerosols within the respiratory tract, especially the alveolar region of the lung. The aerosols formed during welding processes will tend to deposit based on their physical size because diffusion is a major transport mechanism for ultrafine aerosols. Although the aerosol will deposit based upon its physical size, the morphological aspects of the particle will be important in determining its potential toxicity. A partially sintered agglomerate would tend to stay intact upon deposition. In contrast, an open-structured agglomerate, loosely held by van der Waals forces, could de-agglomerate within the pulmonary surfactant.²⁹ As an example, consider the macrophage clearance of a single GMAW particle (Fig. 4b). If this particle de-agglomerated within the pulmonary surfactant, approximately 100 individual particles would have to be cleared. Additionally, the potential that a 5–10 nm primary particle will pass through the pulmonary interstitium is much greater than that of a large agglomerate.³⁰ The de-agglomeration potential of ultrafines represents another salient research topic.

References

- 1 NIOSH Criteria for a Recommended Standard: Welding, Brazing, and Thermal Cutting, 88-110, DHHS, CDC, NIOSH, 1988, pp. 17–22.
- 2 Welding Handbook, L.P. Connor, American Welding Society, Miami, 1987, pp. 1–27.
- 3 Fumes and Gases in the Welding Environment, American Welding Society, Miami, 1979, pp. 6–18.
- 4 P. J. Hewitt, R. Hicks and H. F. Lam, *Ann. Occup. Hyg.*, 1978, **21**, 159.

5 C. N. Gray and P. J. Hewitt, *Ann. Occup. Hyg.*, 1982, **25**, 431.
6 R. R. Heile and D. C. Hill, *Welding J.*, 1975, **54**, 201s.
7 P. J. Hewitt and A. A. Hirst, *Ann. Occup. Hyg.*, 1993, **37**, 297.
8 D. E. Hilton and P. N. Plumridge, *Welding and Metal Fabrication*, 1991, **59**, 555.
9 D. M. Brown, M. R. Wilson, W. MacNee, V. Stone and K. Donaldson, *Toxicol. Appl. Pharmacol.*, 2001, **175**, 191.
10 K. Donaldson, X. Y. Li and W. MacNee, *J. Aerosol Sci.*, 1998, **29**, 553.
11 G. Oberdorster, R. M. Gelein and J. Ferin, *Inhalation Toxicol.*, 1995, **7**, 111.
12 E. L. Cussler, *Diffusion and Mass Transfer in Fluid Systems*, Cambridge University Press, New York, 1995, pp. 325–345.
13 W. B. White, S. M. Johnson and G. B. Dantzig, *J. Chem. Phys.*, 1958, **28**, 751.
14 O. Levenspiel, *Chemical Reaction Engineering*, John Wiley & Sons, New York, 1993, pp. 21–22.
15 C. Y. Wu and P. Biswas, *Combust. Flame*, 1993, **93**, 31.
16 S. K. Durlak, P. Biswas and J. Shi, *J. Hazard. Mater.*, 1997, **56**, 1.
17 T. M. Owens, C. Y. Wu and P. Biswas, *Chem. Eng. Commun.*, 1995, **133**, 31.
18 A. T. Zimmer and P. Biswas, *Am. Ind. Hyg. Assoc. J.*, 2000, **16**, 351.
19 J. A. Seinfeld and S. N. Pandis, *Atmospheric Chemistry and Physics*, John Wiley & Sons, New York, 1998, pp. 547–555.
20 A. T. Zimmer, P. A. Baron and P. Biswas, *J. Aerosol Sci.*, 2002, **33**, 519.
21 A. T. Zimmer, PhD Thesis, University of Cincinnati, Cincinnati, OH, 2000.
22 W. C. Hinds, *Aerosol Technol.*, John Wiley & Sons, New York, 1999, pp. 260–265 and 258–288.
23 A. T. Zimmer and P. Biswas, *J. Aerosol Sci.*, 2001, **32**, 993.
24 R. K. Tandon, R. Payling and B. E. Chenhall, *Appl. Surf. Sci.*, 1985, **20**, 527.
25 V. G. Voitkevich, *Weld. World*, 1988, **26**, 108.
26 P. J. Hewitt and C. N. Gray, *Am. Ind. Hyg. Assoc. J.*, 1983, **44**, 727.
27 P. L. Kalliomaki, J. Grekula, Hagberg and S. Sivonen, *J. Aerosol Sci.*, 1987, **18**, 781.
28 P. Biswas and C. Y. Wu, *J. Air Waste Manag. Assoc.*, 1998, **48**, 113.
29 A. D. Maynard, *Ann. Occup. Hyg.*, 2002, accepted for publication (Suppl. 1).
30 A. Nemmar, P. H. M. Hoet and B. Vanquickenborne, *Circulation*, 2002, **105**, 411.